THE JOURNAL OF BIOLOGICAL CHEMISTRY VOL. 291, NO. 40, pp. 20891–20899, September 30, 2016

The MET/Vascular Endothelial Growth Factor Receptor (VEGFR)-targeted Tyrosine Kinase Inhibitor Also Attenuates FMS-dependent Osteoclast Differentiation and Bone Destruction Induced by Prostate Cancer*

Received for publication, March 31, 2016, and in revised form, August 16, 2016 Published, JBC Papers in Press, August 18, 2016, DOI 10.1074/jbc.M116.727875

Kenta Watanabe[‡1], Michiko Hirata[‡1], Tsukasa Tominari[§], Chiho Matsumoto[‡], Hidenori Fujita[¶], Kazuhiko Yonekura[¶], Gillian Murphy[‖], Hideaki Nagase[§], Chisato Miyaura[‡§], and Masaki Inada[‡§2]**

*From the [‡]Department of Biotechnology and Life Science and [§]Global Innovation Research Organization, Tokyo University of Agriculture and Technology, Tokyo 184-8588, the [¶]Tsukuba Research Center, Taiho Pharmaceutical Co., Ltd., Ibaraki 300-2611, Japan, the [‖]Department of Oncology, University of Cambridge, Cancer Research UK, Cambridge Institute, Li Ka Shing Centre, Cambridge, CB2 0RE, United Kingdom, and the **Kennedy Institute of Rheumatology, Nuffield Department of Orthopaedics, Rheumatology and Musculoskeletal Sciences, University of Oxford, Oxford, OX3 7FY, United Kingdom*

The tyrosine kinase inhibitor TAS-115 that blocks VEGF receptor and hepatocyte growth factor receptor MET signaling exhibits antitumor properties in xenografts of human gastric carcinoma. In this study, we have evaluated the efficacy of TAS-115 in preventing prostate cancer metastasis to the bone and bone destruction using the PC3 cell line. When PC3 cells were injected into proximal tibiae in nude mouse, severe trabecular and cortical bone destruction and subsequent tumor growths were detected. Oral administration of TAS-115 almost completely inhibited both PC3-induced bone loss and PC3 cell proliferation by suppressing osteoclastic bone resorption. In an *ex vivo* bone organ culture, PC3 cells induced osteoclastic bone resorption when co-cultured with calvarial bone, but TAS-115 effectively suppressed the PC3-induced bone destruction. We found that macrophage colony-stimulating factor-dependent macrophage differentiation and subsequent receptor activator of NF-κB ligand-induced osteoclast formation were largely suppressed by adding TAS-115. The phosphorylation of the macrophage colony-stimulating factor receptor FMS and osteoclast related kinases such as ERK and Akt were also suppressed by the presence of TAS-115. Gene expression profiling showed that FMS expression was only seen in macrophage and in the osteoclast cell lineage. Our study indicates that tyrosine kinase signaling in host pre-osteoclasts/osteoclasts is critical for bone destruction induced by tumor cells and that targeting of MET/VEGF receptor/FMS activity makes it a promising therapeutic candidate for the treatment of prostate cancer patients with bone metastasis.

VEGF signaling through the tyrosine kinase receptor VEGF receptor (VEGFR)[3] is a pivotal factor for tumor angiogenesis that regulates tumor progression. However, VEGFR-targeted inhibitor monotherapies showed limited effects on various carcinomas, and even combination therapies with chemotherapeutic agents are unsatisfactory (1, 2). The tyrosine kinase MET is a receptor for hepatocyte growth factor (HGF), and HGF-MET signaling is also involved in tumor progression, metastasis, angiogenesis, and resistance to chemotherapy in various cancers, indicating that MET kinase inhibitors could have major therapeutic potential. Inhibition of both VEGFR and MET signaling pathways has been reported to suppress tumor growth and angiogenesis synergistically (3), suggesting the possibility that the dual inhibition of VEGFR and MET signals may have potential effects on the prevention of tumor growth. Recently, Fujita *et al.* (4) developed a novel VEGFR/MET-targeted tyrosine kinase inhibitor, TAS-115, and showed its antitumor properties in MET-amplified human cancer-bearing mice. In this study, we have investigated the effect of TAS-115 on prostate cancer cell metastasis to bone and a process associated with osteoclast activation.

Bone remodeling is regulated by osteoclastic bone resorption and new bone formation. Osteoclasts, which are the primary bone-resorbing cells, are differentiated from macrophages by a mechanism involving the receptor activator of NF-κB ligand (RANKL) that is expressed on the cell surface of osteoblasts (5, 6). Bone-resorbing factors such as IL-1 act on osteoblasts and induce the expression of RANKL on the cell surface (7, 8). RANKL recognizes RANK, a receptor for RANKL, which is expressed on osteoclast precursors, to induce the differentiation into mature osteoclasts (9). In addition to the differentiation of osteoclasts, the survival of mature osteoclasts and osteoclastic bone resorption are dependent on RANKL, and the lack of RANKL induces the apoptosis of mature osteoclasts

* This work is partly supported by Grants-in-Aid for Scientific Research 25460062 (to C. M.) and 23590069 (to M. I.), National Institute of Health Grant AR40994 (to H. N.), and Global Innovation Research Organization in Tokyo University of Agriculture and Technology (to M. I. and H. N.). This project was also supported by Open Partnership Joint Projects of Japan Society for the Promotion of Science Bilateral Joint Research Projects. The authors declare that they have no conflicts of interest with the contents of this article. The content is solely the responsibility of the authors and does not necessarily represent the official views of the National Institutes of Health.

[1] Both authors contributed equally to this work.

[2] To whom correspondence should be addressed: Dept. of Biotechnology and Life Science, Tokyo University of Agriculture and Technology, 2-24-16 Naka-cho, Koganei, Tokyo 184-8588, Japan. Tel.: 81-42-388-7390; Fax: 81-42-388-7390; E-mail: m-inada@cc.tuat.ac.jp.

[3] The abbreviations used are: VEGFR, vascular endothelial growth factor receptor; HGF, hepatocyte growth factor; M-CSF, macrophage colony-stimulating factor; RANKL, receptor activator of NF-κB ligand; DEXA, dual energy x-ray absorptiometry; TRAP, tartrate-resistant acid phosphatase; qPCR, quantitative PCR; CT, computerized topography; BMD, bone mineral density; sRANKL, soluble RANKL.

(10). Like macrophages, pre-osteoclasts and osteoclasts express FMS (c-*fms*), a receptor for macrophage colony stimulating factor (M-CSF), and M-CSF is essential for the survival and the differentiation of pre-osteoclasts into osteoclast (11).

Prostate cancer has the second highest incidence in men worldwide and is known to frequently induce bone metastasis, accompanied by increased bone resorption and/or sclerotic irregular bone formation in patients with advanced prostate cancer exhibiting chronic pain and pathological fractures (12, 13). Because osteoclastic bone resorption contributes to severe osteolysis during the development of bone metastasis in prostate cancer (14), bisphosphonates such as zoledronic acid have been used for the treatment of bone metastasis in patients with prostate cancer (15), but the outcome of the treatment is still unsatisfactory.

Regarding the possible effects of tyrosine kinase inhibitors in prostate cancer, Dai *et al.* (16) have reported that cabozantinib, a multityrosine kinase inhibitor with activity against MET and VEGFR, inhibited progression of prostate cancer growth *in vivo*. They suggested the possible effectiveness of cabozantinib in both soft tissues and bone sites, but the modulation of bone remodeling by the kinase inhibitor has not been studied. In our previous studies using mouse malignant melanoma B16 and human breast cancer MDA231, we have shown that cell-cell interactions between cancer cells and host osteoblasts could induce RANKL expression in osteoblasts and elicit osteoclastic differentiation and severe bone destruction in the metastatic sites (17, 18). We therefore decided to examine the effects of MET/VEGFR kinase inhibitors on host cells such as osteoblasts and osteoclasts to define the possible role of these kinases in the bone phenotype associated with prostate cancer. For this purpose we used TAS-115, which inhibits both MET and VEGFR, and examined its effects on PC3-induced bone resorption by directly injecting PC3 cells into the proximal medulla of tibiae in nude mouse and by the co-culturing of calvarial bone with PC3 cells *in vitro*. We report here that oral administration of TAS-115 restored bone destruction induced by PC3 mainly by inhibiting the FMS-dependent and RANKL-induced differentiation of pre-osteoclasts into mature osteoclasts.

Results

In Vivo Effect of TAS-115 on the Bone Destruction Induced by Prostate Cancer PC3 Cells—The invasion of prostate cancer cells into bone tissues induces bone destruction by increased bone resorption in the tumor microenvironment. We first investigated the effects of TAS-115, an inhibitor of VEGFR and MET kinases, on the bone destruction induced by PC3 cells *in vivo*. For this series of experiments, we injected PC3 cells into proximal medulla of tibiae in nude mouse with or without oral administration of TAS-115, and bone destruction was measured by micro-CT analysis. As shown in Fig. 1*A*, severe destruction was detected as holes in the surface of cortical bone in the tibiae by 18 days after injection of PC3 cells (Fig. 1*A*, *middle panels*, *white arrows*). In the horizontal section and vertical section, the loss of trabecular bone and destruction holes were detected in the proximal area of tibiae in nude mice injected with PC3 cells (Fig. 1, *B* and *C*, *middle panels*, *white arrows*). Oral administration of TAS-115 almost completely restored the PC3-induced bone loss in both cortical bone and trabecular bone of tibiae in nude mice (Fig. 1, *A–C*, *right panels*). The treatment with TAS-115 for 18 days did not affect body weight in the mice in all experimental groups (data not shown). To confirm the effects of TAS-115 in bone loss, we measured bone mineral density (BMD) by DEXA using respective tibia of the mice. The BMD of the mouse tibiae was

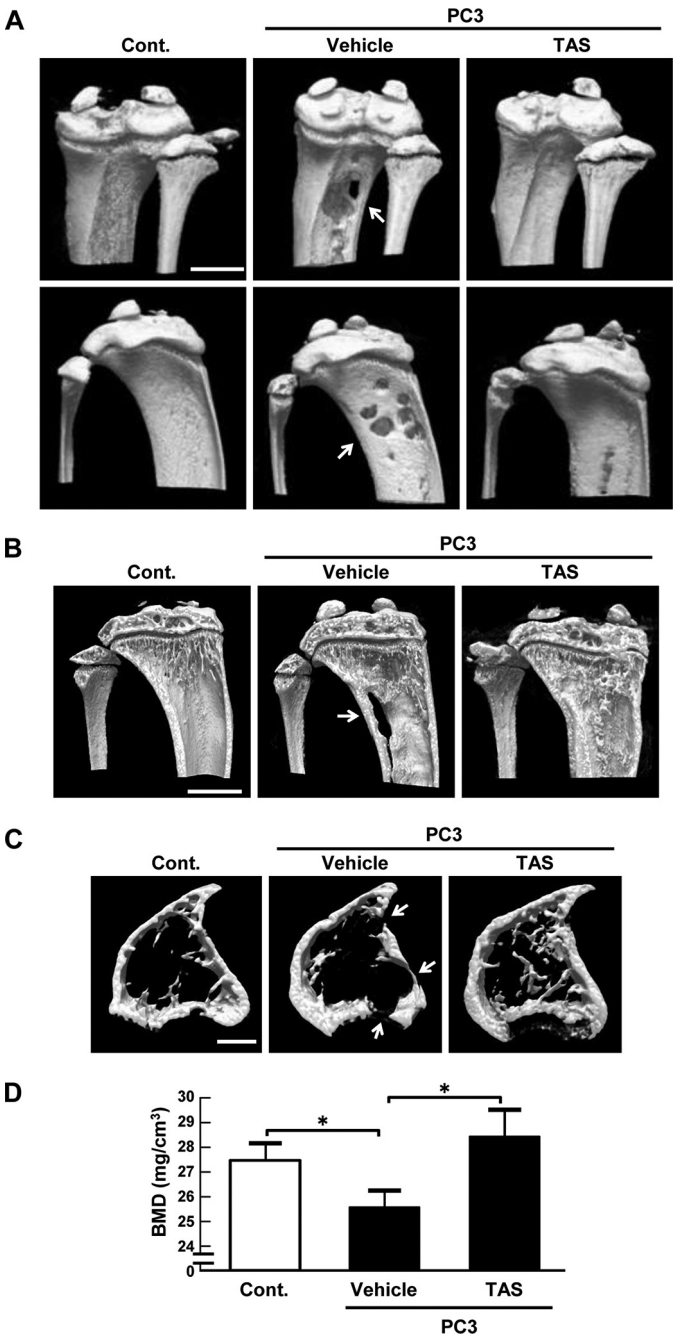

FIGURE 1. **The effect of TAS-115 on the bone resorption in PC3 intra-tibia xenograft model.** Nude mice were injected with or without PC3 cells into the right tibia, and then TAS-115 was administrated orally for 18 days. *A–C*, the tibiae were collected from nude mice, and the three-dimensional images of the tibiae were obtained by micro-CT. *Scale bars*, 2 mm (*A* and *B*) and 0.5 mm (*C*). *D*, BMD of tibiae was evaluated by DEXA. The data are expressed as the means ± S.E. of control ($n = 5$), vehicle ($n = 5$), or TAS-115 ($n = 6$) mice. A significant difference between the two groups is indicated by a *asterisks* (*, $p < 0.05$).

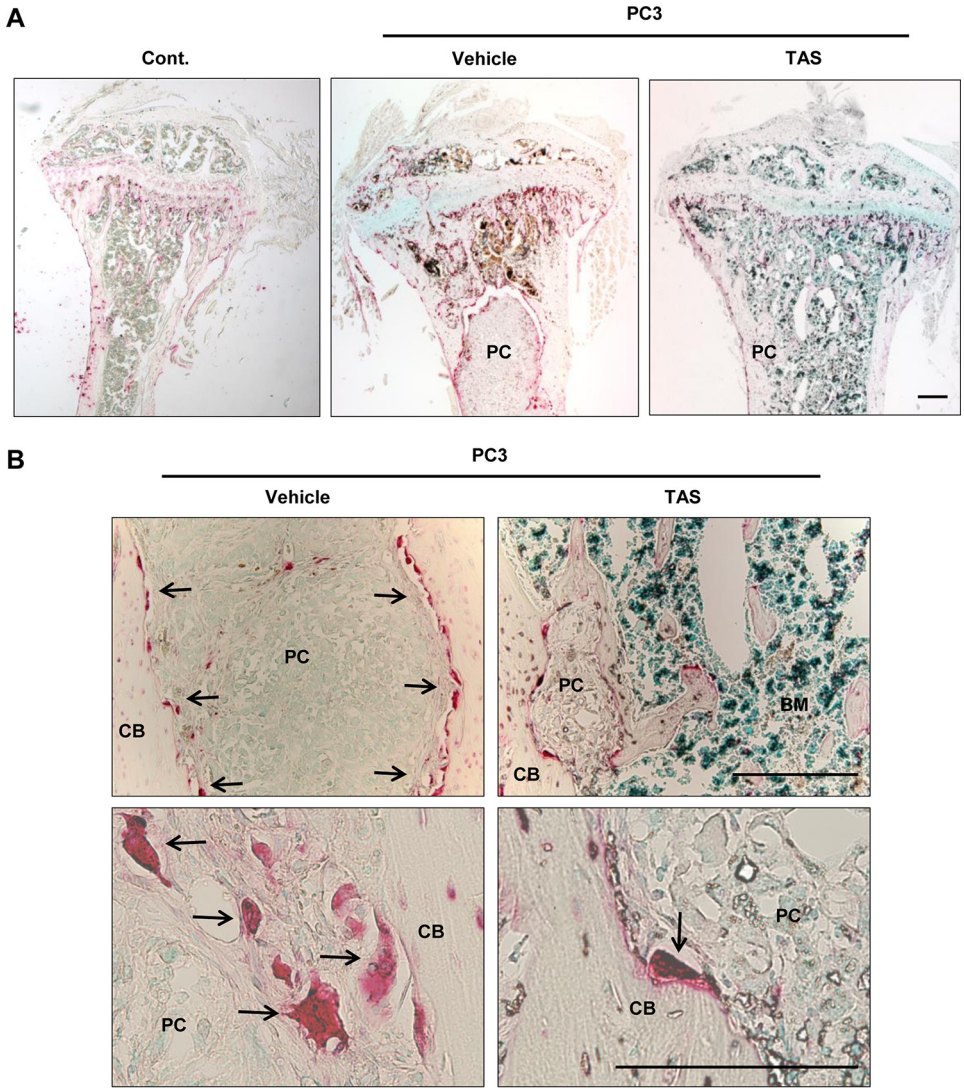

FIGURE 2. **Histological analysis to detect the effect of TAS-115 on the PC3-induced osteoclast formation *in vivo*.** Using the tibiae shown in Fig. 1, the sections were prepared and stained by hematoxylin and eosin and TRAP to detect bone architecture and osteoclasts. *A*, low power magnification. *B*, middle power magnification in *upper panel*, and high power magnification in *lower panel*. *Scale bar*, 300 μm. *TAS*, TAS-115; *PC*, prostate cancer; *CB*, cortical bone; *BM*, bone marrow; *Cont.*, control. *Arrow*, TRAP-positive osteoclast.

decreased in mice injected with PC3, and the decreased bone mass was completely restored by oral administration of TAS-115 (Fig. 1*D*).

For histological analysis, we prepared the section of tibiae, and stained for tartrate-resistant acid phosphatase (TRAP) to detect osteoclasts. In tibiae injected with PC3, the tumor burden was detected in the area of bone marrow and trabecular bone in the proximal region (Fig. 2*A*, *middle panel*), and a large number of active osteoclasts were detected in bone surrounding PC3 tumor (Fig. 2*B*, *upper* and *lower left panels*, *black arrows*). In mice treated with TAS-115, considerably smaller tumors could be detected in the proximal area, TRAP-positive osteoclasts had shrunk to the shape of cells in vehicle mice, and the trabecular bone architecture was normal (Fig. 2, *A* and *B*, *upper* and *lower right panels*, *black arrows*). These results indicate that TAS-115 suppressed both the bone destruction induced by PC3 and the tumor progression in bone tissues.

Effects of TAS-115 on Osteoclastogenesis Induced by Prostate Cancer Cells—The key cellular event required for bone destruction is the formation of osteoclasts. To test the effect of TAS-115 on osteoclastogenesis, we set up an *ex vivo* organ cultures, where calvariae were co-cultured with PC3 cells. Numerous TRAP-positive osteoclasts were observed in this co-culture system (Fig. 3*A*, *upper middle panel*), but in the presence of TAS-115, osteoclast formation was almost completely abrogated (Fig. 3*A*, *upper right panel*). Micro-CT analysis of calvariae showed severe osteoclastic bone resorption lacuna in the co-cultures of PC3 cells and calvariae (Fig. 3*A*, *lower middle panel*), but the treatment with TAS-115 inhibited the bone resorption (Fig. 3*A*, *lower right panel*). When bone resorbing activity was monitored by measuring the calcium level in the culture media, we confirmed that PC3 cells induced bone resorbing activity and that TAS-115 dose-dependently suppressed the activity (Fig. 3*B*). The mRNA expression of osteoclast markers, such as cathepsin K, TRAP, FMS, and RANK, was greatly elevated in

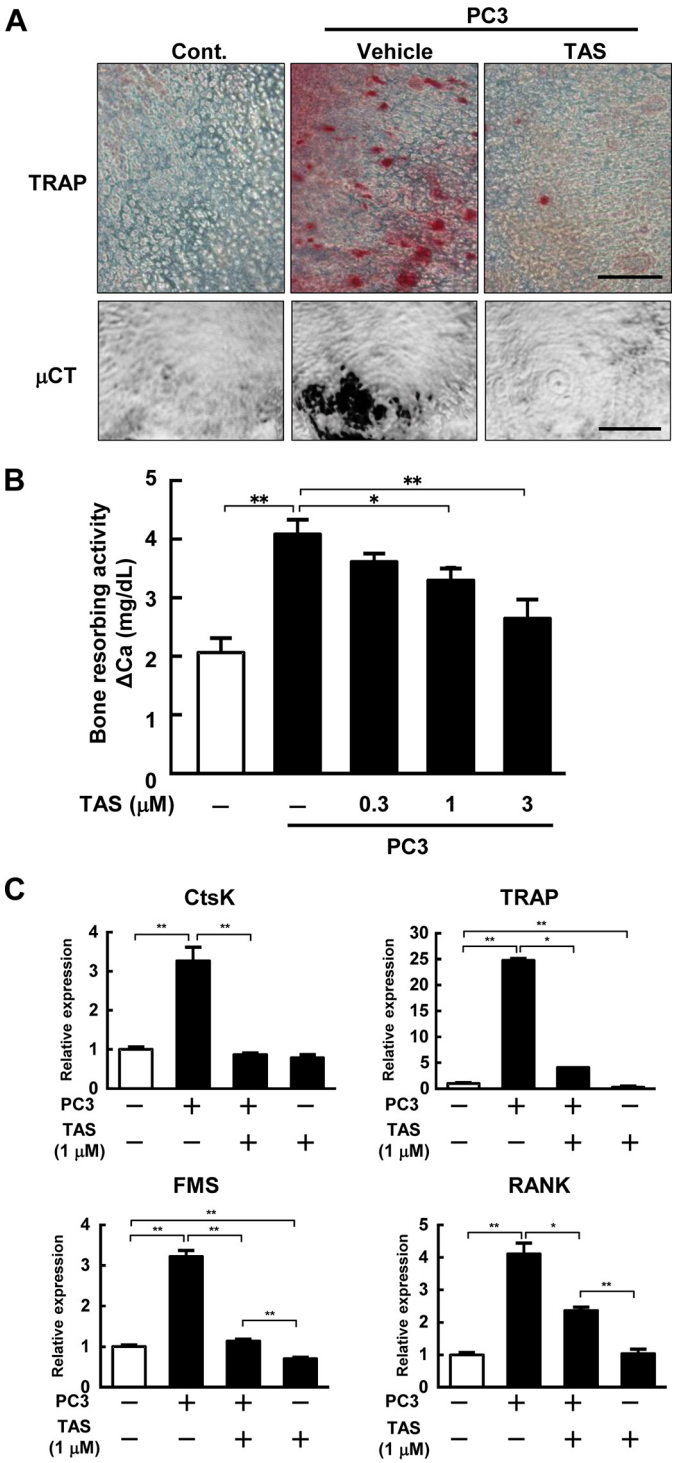

FIGURE 3. **The effect of TAS-115 on the PC3-induced bone resorption.** *A*, the calvariae were cultured for 5 days with or without PC3 cells in the presence or absence of TAS-115 (1 μM) and stained with TRAP. By micro-CT, the PC3-induced bone destruction was detected. The *scale bar* in the *upper panels* indicated 200 μm, and that in the *lower panels* indicated 1 mm. *B*, the bone resorbing activity was evaluated by measuring the medium calcium in the culture of calvariae with or without PC3 cells in the presence or absence of TAS-115 (0.3, 1, and 3 μM). The data are expressed as the means ± S.E. of four independent wells. A significant difference between the two groups is indicated by *asterisks* (*, $p < 0.01$; **, $p < 0.001$). *C*, the mRNA expression of mouse TRAP, cathepsin K, FMS, and RANK were detected by qPCR in the calvarial cultures. The data are expressed as the means ± S.E. of three independent wells. A significant difference between the two groups is indicated by *asterisks* (*, $p < 0.01$; **, $p < 0.001$). *Cont.*, control. *TAS*, TAS-115.

calvariae in the presence of PC3 cells and was clearly suppressed by adding TAS-115 (Fig. 3*C*). In control cultures without PC3, TAS-115 did not affect the bone resorbing activity (data not shown).

M-CSF-dependent Macrophage Differentiation and Osteoclast Formation Are Suppressed by TAS-115—To identify target cells for TAS-115 in the prostate cancer-induced osteoclast differentiation and bone resorption, we used cultures of bone marrow macrophages, which could differentiate into mature osteoclasts by treatment with M-CSF and soluble RANKL (sRANKL). Pre-osteoclasts have been reported as adherent cells after treatment with M-CSF (19). When mouse bone marrow cells were cultured for 5 days in the presence of M-CSF, most cells with strong adherence to the dish surface were positive with a mouse macrophage marker F4/80 (Fig. 4*A*). In these cultures, the addition of TAS-115 completely suppressed the M-CSF-dependent macrophage differentiation (Fig. 4*A*). After 5 days of culture with M-CSF, the addition of sRANKL for the following 5 days induced the differentiation into mature osteoclasts in the presence of M-CSF (Fig. 4*B*). Adding TAS-115 completely suppressed the osteoclast differentiation from bone marrow macrophages to pre-osteoclasts in the presence of sRANKL and M-CSF (Fig. 4*B*). Therefore, bone marrow macrophages and pre-osteoclasts were potential target cells for TAS-115, and the effects on bone resorption appears to be elicited by the suppressive effects on the M-CSF-dependent differentiation from osteoclast precursors into mature osteoclasts.

M-CSF-induced Phosphorylation of FMS, AKT, and ERK in Osteoclasts Is Inhibited by TAS-115—Using mouse osteoclasts differentiated from bone marrow macrophages (19), we examined the M-CSF-induced phosphorylation of FMS and its related signal molecules of AKT and ERK. In Western blot analysis, the phosphorylation of FMS detected by antibody against pFMS was greatly elevated by adding M-CSF to osteoclasts, and the expression was dose-dependently suppressed by TAS-115 (Fig. 5). The levels of AKT and ERK phosphorylation were also elevated by M-CSF and suppressed by TAS-115, suggesting that the tyrosine kinase FMS may influence the subsequent signaling pathway involving AKT and ERK. FMS signaling may be a critical target for TAS-115 in the regulation of the M-CSF-dependent differentiation and survival of pre-osteoclasts and osteoclasts.

RT-PCR analysis of mouse primary osteoblasts, bone marrow-derived macrophages, osteoclasts, and PC3 cells indicated that bone marrow macrophages cultured with M-CSF expressed HGF, MET, VEGF-A, VEGFR2, M-CSF, and FMS mRNAs, and the expression of VEGF-A mRNA was elevated in osteoclasts induced by adding sRANKL to macrophages (Fig. 6). In PC3 cells, we detected the mRNA expression of HGF, MET, VEGF-A, VEGFR2, RANK, and M-CSF, suggesting that VEGFR and MET signals may regulate growth and cell function in prostate cancer cells PC3 (Fig. 6). FMS expression was only seen in macrophage and osteoclast lineage of the cells, supporting the notion that the M-CSF/FMS signaling is essential for macrophage/osteoclast differentiation.

To examine the direct effects of TAS-115 on the proliferation of PC3 cells, PC3 cells were treated with TAS-115 in the cul-

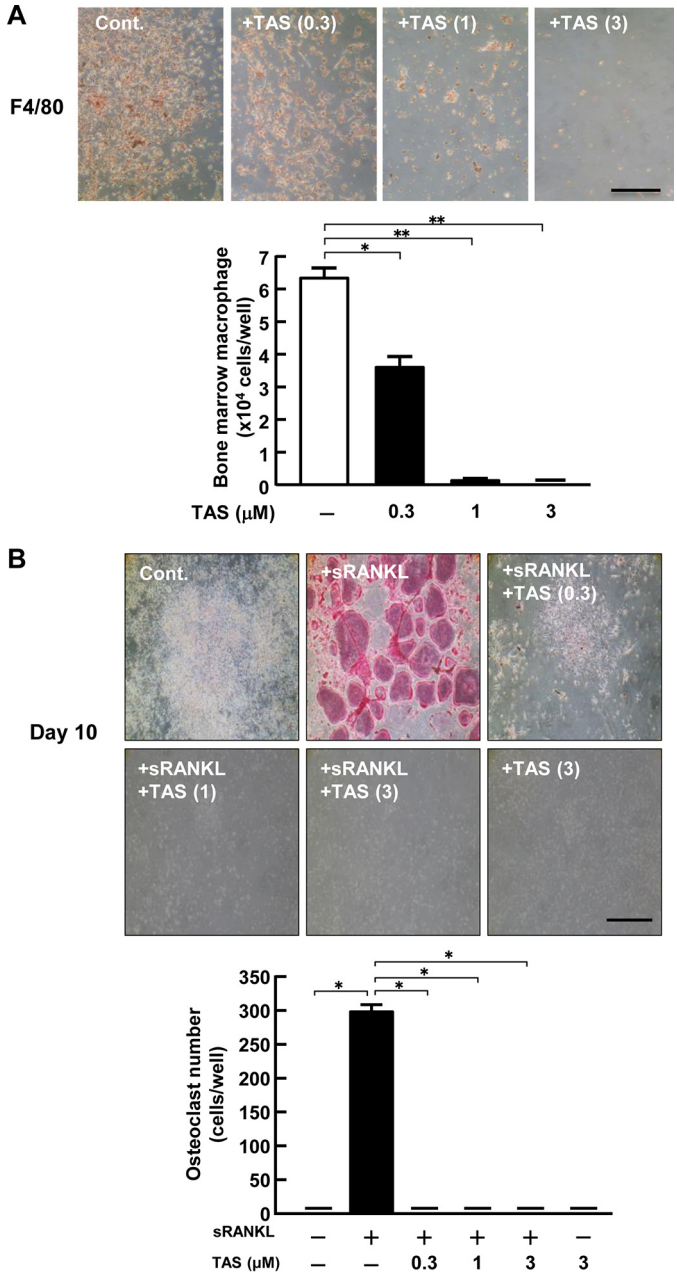

FIGURE 4. **The effect of TAS-115 on the M-CSF-dependent macrophage differentiation and osteoclasts formation.** *A*, bone marrow cells were cultured for 5 days in M-CSF with or without TAS-115 (0.3, 1, and 3 μM). After the culture, the adherent cells were stained with a macrophage marker F4/80 using anti-F4/80 antibody in immunostaining. The number of cells adhered to dish surface was counted as pre-osteoclasts. The data are expressed as the means ± S.E. of four independent wells. A significant difference between the two groups is indicated by *asterisks* (*, $p < 0.01$; **, $p < 0.001$). *Scale bar*, 250 μm. *B*, bone marrow cells were cultured for 5 days with M-CSF to generate macrophages and then treated with or without TAS-115 (0.3, 1, and 3 μM) and then treated M-CSF and sRANKL (100 ng/ml) for 5 days. After the culture, the cells adhering to the well surface were stained for TRAP. The number of TRAP-positive cells was counted. The data are expressed as the means ± S.E. of four independent wells. A significant difference between the two groups is indicated by *asterisks* (*, $p < 0.001$). *Scale bar*, 250 μm. *Cont.*, control. *TAS*, TAS-115.

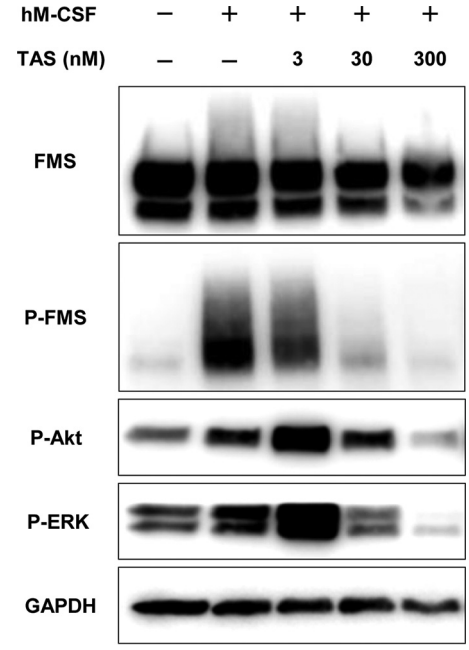

FIGURE 5. **The effect of TAS-115 on the FMS signaling pathway in osteoclasts.** Osteoclasts derived from bone marrow macrophages were treated with M-CSF (100 ng/ml) in the presence or absence of TAS-115 (3, 30, and 300 nM). After 1 min, the total protein was collected and subjected to Western blotting to detect the phosphorylation of FMS, Akt, and ERK.

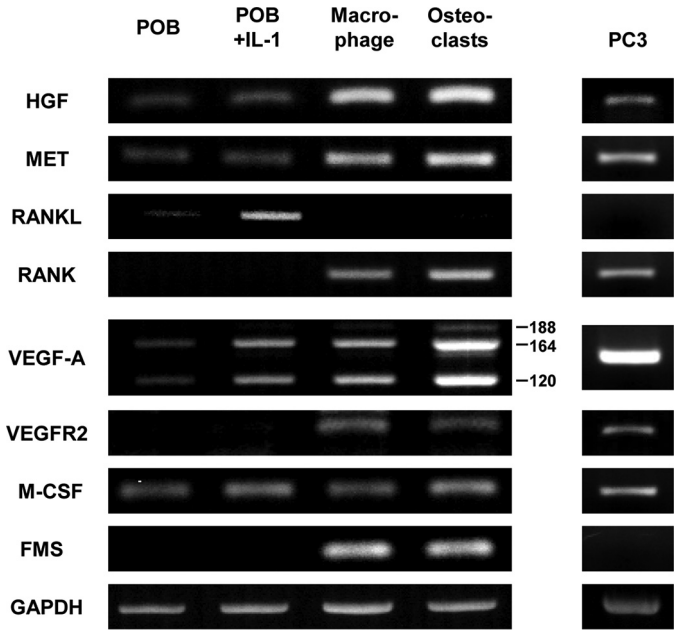

FIGURE 6. **The mRNA expression of HGF, MET, RANKL, RANK, VEGF-A, VEGFR2, M-CSF, and FMS in mouse primary osteoblasts, mouse bone marrow microphages, osteoclasts, and PC3 cells.** Mouse primary osteoblasts (*POB*) were cultured for 24 h in the presence or absence of IL-1 (2 ng/ml). Mouse bone marrow cells were cultured for 5 days with M-CSF (100 ng/ml) and then treated with M-CSF and sRANKL (100 ng/ml) for 5 days. The total RNA was extracted, and the expression of HGF, MET, RANKL, RANK, VEGF-A, VEGFR2, M-CSF, and FMS mRNAs was detected by RT-PCR.

tures. TAS-115 significantly suppressed the cell growth of PC3 *in vitro* (Fig. 7*A*).

Discussion

In the present study, we have shown that oral administration of the tyrosine kinase inhibitor TAS-115 exhibits profound anti-tumor activity *in vivo* using a bone metastasis model of human prostate cancer cells PC3 in nude mice. Bone destruction with increased osteoclastic bone resorption was abolished, and the PC3 tumor volume in the bone was dramatically suppressed by TAS-115 treatment. Previous studies have shown

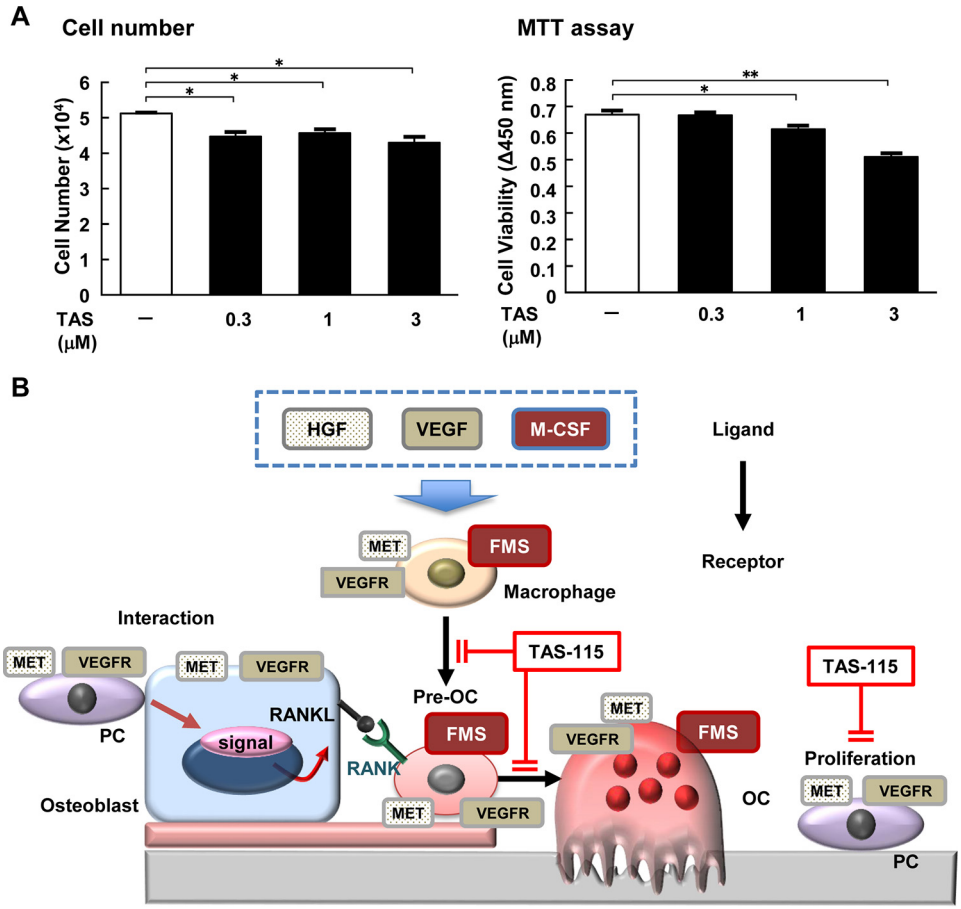

FIGURE 7. **The mechanism of the growth and bone metastasis of PC3, and the suppressive effects of TAS-115 in bone tissues.** *A*, the effect of TAS-115 on the proliferation of PC3 cells *in vitro*. PC3 cells were cultured for 3 days with or without TAS-115 (0.3, 1, and 3 μM). The number of PC3 cells was counted using Cell Counting Kit 8 (*left panel*). 3-(4,5-Dimethylthiazol-2-yl)-2,5-diphenyltetrazolium bromide (*MTT*) assay was used to detect cell viability (*right panel*). The data are expressed as the means ± S.E. of five independent wells. A significant difference between the two groups is indicated by *asterisks* (*, $p < 0.01$; **, $p < 0.001$. *B*, a schematic model of osteoclastogenesis induced by prostate cancer cells, and the mechanism of suppressive effects of TAS-115. All macrophages, pre-osteoclasts, osteoclasts, osteoblasts, and PC3 cells produce the growth factors (HGF, VEGF, and M-CSF). TAS-115 suppresses FMS-dependent signal in pre-osteoclasts and osteoclasts by inhibiting the phosphorylation of FMS. TAS-115 also acts on tumor cells PC3 and suppresses cell growth. The action of TAS-115 may be elicited by the suppression of FMS-regulated osteoclastogenesis and MET/VEGFR-dependent cancer cell proliferation in tumor microenvironments of bone tissues.

that TAS-115 is an efficient MET/VEGFR inhibitor (4). Indeed, TAS-115 acted directly on PC3 cells and partly suppressed the cell growth *in vitro* (Fig. 7*A*). Analysis of mRNA expression patterns in *in vitro* cell culture showed that PC3 cells expressed HGF, MET, VEGF-A, VEGFR2, RANK, and M-CSF, suggesting that VEGFR2 and MET signaling may regulate their growth and function. The expression of RANKL mRNA was not detected in PC3 cells (Fig. 6). Although osteoblasts also express HGF, MET, and VEGF-A at low levels (Fig. 6), the role of VEGFR/MET signaling in osteoblasts is not clear. Nonetheless, TAS-115 did not influence the expression of the osteoclast differentiation factor, RANKL by osteoblasts (data not shown).

Because tumor progression in bone is closely related to the bone resorption induced by cancer cells in the tumor microenvironment, we hypothesized that the suppression of osteoclastogenesis by the abrogation of tyrosine kinase activity of growth factor receptor is likely to be a key mechanism for the action of TAS-115 in prostate cancer growth in bone tissues. Almost complete TAS-115-mediated suppression of TRAP staining both in the *in vivo* model and in calvariae cultured with PC3 cells described here supports this concept. Further, bone marrow macrophages and osteoclasts differentiated from bone marrow cells *in vitro* were found to express mRNAs for MET and VEGFR2, as well as FMS. TAS-115 treatment of macrophages in culture suppressed the phosphorylation of FMS as well as downstream kinases. M-CSF is essential for the growth, differentiation, and survival of monocyte macrophages, pre-osteoclasts, and osteoclasts. From these results, we conclude that TAS-115 acts on osteoclast precursors by suppressing the FMS-dependent signaling.

Fig. 7*B* shows a scheme covering all the potential levels of TAS-115 function in the abrogation of the development of bone metastases by prostate cancer cells. All macrophages, pre-osteoclasts, osteoclasts, osteoblasts, and PC3 cells produce the growth factors (HGF, VEGF, and M-CSF). TAS-115 suppresses FMS-dependent signal in pre-osteoclasts and osteoclasts by inhibiting the phosphorylation of FMS. Several targets for TAS-115 were identified in a ProfilerPro kinase screen (4). However, it is well known that null mutation of FMS induces osteopetrosis because of the lack of osteoclast in *op/op* mice (20). We therefore concluded that FMS is a crucial target for TAS-115 as tyrosine kinase inhibitor, which suppresses osteoclast differentiation medi-

ated by PC3 in bone. TAS-115 also acts on tumor cells PC3 and suppresses cell growth. Previous studies have shown that PC3 produces parathyroid hormone-related peptides (21) and that it is involved in cell migration of PC3 *in vitro* (22), but the roles of parathyroid hormone-related peptides in the growth and bone metastasis of PC3 *in vivo* are not known. The action of TAS-115 may be elicited by the suppression of FMS-regulated osteoclastogenesis and MET/VEGFR-dependent cancer cell proliferation in tumor microenvironments of bone tissues.

In osteoclastogenesis, RANK signaling in osteoclast precursors results in the recruitment of TRAF6, which activates NF-κB, and induces an AP-1 component c-Fos, which contributes to the nuclear translocation of NFATc1, the master transcription factor for osteoclast differentiation (23, 24). TRAF6 also activates calcium signaling, which may be essential for the auto-amplification and activation of NFATc1 in pre-osteoclasts (25). On the other hand, M-CSF/FMS signal activates tyrosine kinases involving MAP kinase cascade (26). The relationship between the RANK signal and the FMS signaling pathway is not clear. Arai *et al.* (27) have reported that M-CSF upregulates RANK expression in macrophages, indicating a possible interaction between TRAF6 and FMS. Further studies are needed to define the relationship between TRAF6 and FMS signaling in pre-osteoclasts and osteoclasts.

Targeting the receptor tyrosine kinase signaling pathways is one of the strategies for the new drug development for cancer. Sulpice *et al.* (28) have reported that VEGF and HGF cooperatively activate intracellular signaling involving MAPK in endothelial cells and promote neovascularization. In cancer cells, HGF and MET signaling elicit the activation of AKT, MAPK, and RAP1, which are essential for cell cycle progression and cytoskeletal changes (29). For the inhibition of HGF/MET activation in cancer patients, various MET antagonist and MET kinase inhibitors are now in clinical trials (29), but the effects of these agents on bone metastasis are not known. It was reported that treatment with TAS-115 gives relatively selective inhibition of VEGFR and MET with marked anti-tumor activity and low toxicity in *in vivo* model of tumor progression (4). The current study shows that the additional inhibition of the tyrosine kinase FMS by TAS-115 has profound effects on prostate cancer-driven osteoclastogenesis, and its proliferation extends the capability of this agent to act as a powerful antidote to the devastating effects of metastatic spread to bone.

Experimental Procedures

Animals, Cells, and Reagents—BALB/c nu/nu nude mice, and newborn *ddy* mice were obtained from Japan SLC Inc. (Shizuoka, Japan). All procedures were performed in accordance with institutional guidelines for animal research at the Tokyo University of Agriculture and Technology. PC3, a human prostate cancer cell line, was obtained from American Type Culture Collection, and we isolated a clone which consistently underwent a high frequency of bone metastasis. PC3 cells were cultured in RPMI 1640 medium with 10% FBS at 37 °C under 5% CO_2 in air. TAS-115, a VEGFR/MET-targeted kinase inhibitor, was prepared by Taiho Pharmaceutical Co., Ltd. (Tokyo Japan) as reported previously (4).

Culture of Primary Osteoblastic Cells—Primary osteoblastic cells were isolated from 2-day-old mouse calvariae, as described previously (30). Osteoblastic cells were cultured in α-modified minimum essential medium with 10% FBS at 37 °C under 5% CO_2 in air.

Differentiation of Bone Marrow Macrophages into Pre-osteoclasts and Osteoclasts—Bone marrow cells (3×10^6 cells) were isolated from 6-week-old mouse tibiae, cultured for 5 days with M-CSF (100 ng/ml) to generate macrophages, and cultured for another 5 days with sRANKL (100 ng/ml) to induce differentiation into osteoclasts, as reported (19, 31). After 10 days of culture, the TRAP-positive multinucleated cells containing three or more nuclei/cell were counted as osteoclasts. To monitor the number of pre-osteoclasts, bone marrow cells were cultured for 5 days with M-CSF. Pre-osteoclasts which strongly adhere to the dish surface were monitored by pipetting away non-adherent cells and the counting of adherent cells, as reported (19, 31). The adherent cells were stained with a macrophage marker F4/80 using anti-F4/80 antibody (Santa Cruz Biotechnology, SC-25830) in immunostaining. To detect the antibody, HRP/AEC method was used following manufactured company's instructions (ab93686; Abcam).

Co-culture of Mouse Calvaria and PC3 Cells for Monitoring Bone Resorbing Activity—Mouse calvariae were isolated from 5-day-old mice, dissected in half, and cultured for 24 h in BGJb containing 1 mg/ml of BSA. Calvariae were co-cultured with PC3 cells with or without TAS-115 for 5 days. The bone resorbing activity was evaluated by measuring the concentration of calcium in the conditioned medium (32). The calvariae cultured for 5 days were fixed by 70% ethanol and stained with TRAP to detect osteoclasts.

RT-PCR Analysis and Quantitative PCR—Total RNA was extracted from cultured cells, bone marrow-derived cells, PC3 cells, and calvariae cultured with or without PC3, and cDNA was synthesized from total RNA. For RT-PCR, cDNA was amplified by PCR using respective PCR primers. The PCR product was run on a 1.5% agarose gel and stained with ethidium bromide. The qPCR was performed with iQ SYBR Green Supermix (Bio-Rad). The primers for respective mouse and human genes used in RT-PCR and qPCR are shown in Table 1.

Injection of PC3 Cells into Tibiae in Nude Mice—PC3 cells (1×10^5 cell) were injected into the proximal medulla of the right tibiae in 6-week-old nude mice, and tibiae were collected from mice on day 18. Some of the mice were administered orally with TAS-115 (50 mg/kg of body weight/day). As a vehicle group, the mice were administered with distilled water. Control mice were injected with PBS without PC3 cells. The tibiae were used for micro-CT scanning, DEXA, and histological analysis. The tibiae were collected from nude mice and decalcified using EDTA for 14 days and embedded in paraffin, and the sections were prepared and stained by hematoxylin and eosin and TRAP to detect osteoclasts.

DEXA and Micro-CT Analysis—The BMD of the tibiae was measured by dual x-ray absorptiometry (model DCS-600R; Aloka). The bone mineral content of the femurs was closely correlated with the ash weight. The BMD was calculated by dividing the bone mineral content of the measured area by the area. CT scanning of the tibiae and calvariae was performed using a microfocus x-ray CT system (R_mCT2; Rigaku and SMX-90T; Shimadzu), and three-dimensional microstructural

TABLE 1
The primer sets for various genes used in RT-PCR and qPCR

Gene	Forward	Reverse
Mouse HGF	5′-agagaggcgaggagaagcgca-3′	5′-tccagtgtagccccagccgta-3′
Human HGF	5′-cagcaccatgtgggtgac-3′	5′-tcttttcctttgtccctctgc-3′
Mouse MET	5′-ggcccgtgttggaacaccca-3′	5′-catgccgctggcaagtccct-3′
Human MET	5′-gcaggaaggaactttacagtgg-3′	5′-gttgcagattcagctgttgc-3′
Mouse RANKL	5′-aggctgggccaagatctcta-3′	5′-gtctgtaggtacgcttcccg-3′
Human RANKL	5′-tgattcatgtaggagaattaaacagg-3′	5′-gatgtgctgtgatccaacga-3′
Mouse RANK	5′-tgcgtgctgctcgttcca-3′	5′-tgccaggatccaccgccaccag-3′
Human RANK	5′-gcaggtggctttgcagat-3′	5′-gcatttagaagacatgtactttcctg-3′
Mouse VEGF-A	5′-ctgctctcttgggtgcactgg-3′	5′-caccgccttggcttgtcacat-3′
Human VEGF-A	5′-cctccgaaaccatgaacttt-3′	5′-atgattctgccctcctcctt-3′
Mouse VEGFR2	5′-tgcctacctcacctgtttcc-3′	5′-ctctttcgcttactgttctggag-3′
Human VEGFR2	5′-cagcatcaccagtagccaga-3′	5′-tccttatacagatcttcaggagctt-3′
Mouse M-CSF	5′-ctgctgctggtctgtctcct-3′	5′-tgaagtctccatttgactgtcg-3′
Human M-CSF	5′-gcagctgcaggaactctctt-3′	5′-tccagcaactggagaggtg-3′
Mouse FMS	5′-cagtacttcagggccgtctc-3′	5′-caccagcagagacatgacaga-3′
Human FMS	5′-gaacatccacctcgagaagaaa-3′	5′-gacaggcctcatctccacat-3′
Mouse CtsK	5′-gcctagcgaacagattctcaa-3′	5′-cactgggtgtccagcattt-3′
Mouse TRAP	5′-cttccccagcccttactacc-3′	5′-gagttgccacacagcatcac-3′

image data were reconstructed using the software program as reported previously (17).

Cell Proliferation Assays—PC3 cells (1×10^4 cells) were cultured for 3 days with or without TAS-115, and the number of cells was counted. PC3 cells (2×10^3 cells) were cultured for 3 days with or without TAS-115, and the cell viability was measured using Cell Counting Kit 8 (Dojindo). The 3-(4,5-dimethylthiazol-2-yl)-2,5-diphenyltetrazolium bromide assay was also used to monitor cell proliferation.

Phosphorylation Analysis by Western Blotting—Osteoclasts differentiated from bone marrow macrophages were treated for 1 min with or without TAS-115 and lysed in cell extraction buffer (Thermo Fisher Scientific) containing phosphatase inhibitor (PhosSTOP; Roche) and protease inhibitor (Complete in EASYPack; Roche). The cell lysates were centrifuged at $12{,}000 \times g$ for 10 min, and supernatants were collected. The protein concentration of the supernatant was examined by BCA assay (BCA protein assay kit; Thermo Fisher Scientific). Samples (10 μg) were subjected to SDS-PAGE and transferred onto PVDF membranes. Membranes were blocked with 5% BSA in TBS-T (TBS with 0.05% Tween 20) and incubated with primary antibodies. After washing three time with TBS-T, membranes were incubated with the corresponding secondary antibody in 1% BSA in TBS-T and developed with SuperSignal West Femto (Thermo Fisher Scientific) by ChemiDoc XRS+ (Bio-Rad). Antibodies against phospho-FMS (Tyr^{723}), phospho-Akt (Ser^{473}), phospho-ERK (Thr^{202}/Tyr^{204}), and GAPDH antibody were purchased from Cell Signaling; anti-FMS antibody was from Santa Cruz.

Statistical Analysis—The data are expressed as the means ± S.E. The significance of differences was analyzed using Student's *t* test.

Author Contributions—M. I., C. M., and M. H. conceived and designed the experiments; K. W., M. I., C. M., and H. F. developed the methodology; K. W., T. T., and C. M. acquired the data (provided animals, provided facilities, etc.); M. I., C. M., K. W., M. H., and K. Y. analyzed and interpreted the data; and M. I., C. M., K. W., M. H., G. M., and H. N. wrote and reviewed the manuscript.

Acknowledgment—We thank Wakana Kaizuka for expert assistance.

References

1. Bergh, J., Bondarenko, I. M., Lichinitser, M. R., Liljegren, A., Greil, R., Voytko, N. L., Makhson, A. N., Cortes, J., Lortholary, A., Bischoff, J., Chan, A., Delaloge, S., Huang, X., Kern, K. A., *et al.* (2012) First-line treatment of advanced breast cancer with sunitinib in combination with docetaxel versus docetaxel alone: results of a prospective, randomized phase III study. *J. Clin. Oncol.* **30,** 921–929
2. Teoh, D., and Secord, A. A. (2012) Antiangiogenic agents in combination with chemotherapy for the treatment of epithelial ovarian cancer. *Int. J. Gynecol. Cancer* **22,** 348–359
3. Eswaraka, J., Giddabasappa, A., Han, G., Lalwani, K., Eisele, K., Feng, Z., Affolter, T., Christensen, J., and Li, G. (2014) Axitinib and crizotinib combination therapy inhibits bone loss in a mouse model of castration resistant prostate cancer. *BMC Cancer* **14,** 742–751
4. Fujita, H., Miyadera, K., Kato, M., Fujioka, Y., Ochiiwa, H., Huang, J., Ito, K., Aoyagi, Y., Takenaka, T., Suzuki, T., Ito, S., Hashimoto, A., Suefuji, T., Egami, K., Kazuno, H., *et al.* (2013) The novel VEGF receptor/MET-targeted kinase inhibitor TAS-115 has marked *in vivo* antitumor properties and a favorable tolerability profile. *Mol. Cancer Ther.* **12,** 2685–2696
5. Wong, B. R., Rho, J., Arron, J., Robinson, E., Orlinick, J., Chao, M., Kalachikov, S., Cayani, E., Bartlett, F. S., 3rd, Frankel, W. N., Lee, S. Y., and Choi, Y. (1997) TRANCE is a novel ligand of the tumor necrosis factor receptor family that activates c-Jun N-terminal kinase in T cells. *J. Biol. Chem.* **272,** 25190–25194
6. Yasuda, H., Shima, N., Nakagawa, N., Yamaguchi, K., Kinosaki, M., Mochizuki, S., Tomoyasu, A., Yano, K., Goto, M., Murakami, A., Tsuda, E., Morinaga, T., Higashio, K., Udagawa, N., Takahashi, N., *et al.* (1998) Osteoclast differentiation factor is a ligand for osteoprotegerin/osteoclastogenesis-inhibitory factor and is identical to TRANCE/RANKL. *Proc. Natl. Acad. Sci. U.S.A.* **95,** 3597–3602
7. Morony, S., Capparelli, C., Sarosi, I., Lacey, D. L., Dunstan, C. R., and Kostenuik, P. J. (2001) Osteoprotegerin inhibits osteolysis and decreases skeletal tumor burden in syngeneic and nude mouse models of experimental bone metastasis. *Cancer Res.* **61,** 4432–4436
8. Lacey, D. L., Timms, E., Tan, H. L., Kelley, M. J., Dunstan, C. R., Burgess, T., Elliott, R., Colombero, A., Elliott, G., Scully, S., Hsu, H., Sullivan, J., Hawkins, N., Davy, E., Capparelli, C., *et al.* (1998) Osteoprotegerin ligand is a cytokine that regulates osteoclast differentiation and activation. *Cell* **93,** 165–176
9. Suda, T., Takahashi, N., Udagawa, N., Jimi, E., Gillespie, M. T., and Martin, T. J. (1999) Modulation of osteoclast differentiation and function by the new members of the tumor necrosis factor receptor and ligand families. *Endocr. Rev.* **20,** 345–357
10. Boyce, B. F., and Xing, L. (2008) Functions of RANKL/RANK/OPG in bone modeling and remodeling. *Arch. Biochem. Biophys.* **473,** 139–146
11. Feng, X., and Teitelbaum, S. L. (2013) Osteoclasts: new insights. *Bone Res.* **1,** 11–26

12. Olechnowicz, S. W., and Edwards, C. M. (2014) Contributions of the host microenvironment to cancer-induced bone disease. *Cancer Res.* **74,** 1625–1631
13. Israeli, R. S. (2008) Managing bone loss and bone metastases in prostate cancer patients: a focus on bisphosphonate therapy. *Rev. Urol.* **10,** 99–110
14. Zhang, J., Dai, J., Qi, Y., Lin, D. L., Smith, P., Strayhorn, C., Mizokami, A., Fu, Z., Westman, J., and Keller, E. T. (2001) Osteoprotegerin inhibits prostate cancer-induced osteoclastogenesis and prevents prostate tumor growth in the bone. *J. Clin. Invest.* **107,** 1235–1244
15. Gartrell, B. A., and Saad, F. (2014) Managing bone metastases and reducing skeletal related events in prostate cancer. *Nat. Rev. Clin. Oncol.* **11,** 335–345
16. Dai, J., Zhang, H., Karatsinides, A., Keller, J. M., Kozloff, K. M., Aftab, D. T., Schimmoller, F., and Keller, E. T. (2014) Cabozantinib inhibits prostate cancer growth and prevents tumor-induced bone lesions. *Clin. Cancer Res.* **20,** 617–630
17. Inada, M., Takita, M., Yokoyama, S., Watanabe, K., Tominari, T., Matsumoto, C., Hirata, M., Maru, Y., Maruyama, T., Sugimoto, Y., Narumiya, S., Uematsu, S., Akira, S., Murphy, G., Nagase, H., *et al.* (2015) Direct melanoma cell contact induces stromal cell autocrine prostaglandin E2-EP4 receptor signaling that drives tumor growth, angiogenesis and metastasis. *J. Biol. Chem.* **290,** 29781–29793
18. Ohshiba, T., Miyaura, C., Inada, M., and Ito, A. (2003) Role of RANKL-induced osteoclast formation and MMP-dependent matrix degradation in bone destruction by breast cancer metastasis. *Br. J. Cancer* **88,** 1318–1326
19. Kobayashi, K., Takahashi, N., Jimi, E., Udagawa, N., Takami, M., Kotake, S., Nakagawa, N., Kinosaki, M., Yamaguchi, K., Shima, N., Yasuda, H., Morinaga, T., Higashio, K., Martin, T. J., and Suda, T. (2000) Tumor necrosis factor α stimulates osteoclast differentiation by a mechanism independent of the ODF/RANKL-RANK interaction. *J. Exp. Med.* **191,** 275–286
20. Wiktor-Jedrzejczak, W., Bartocci, A., Ferrante, A. W., Jr., Ahmed-Ansari, A., Sell, K. W., Pollard, J. W., and Stanley, E. R. (1990) Total absence of colony-stimulating factor 1 in the macrophage-deficient osteopetrotic (op/op) mouse. *Proc. Natl. Acad. Sci. U.S.A.* **87,** 4828–4832
21. Ongkeko, W. M., Burton, D., Kiang, A., Abhold, E., Kuo, S. Z., Rahimy, E., Yang, M., Hoffman, R. M., Wang-Rodriguez, J., and Deftos, L. J. (2014) Parathyroid hormone related-protein promotes epithelial-to-mesenchymal transition in prostate cancer. *PLoS One* **9,** e85803
22. Bhatia, V., Mula, R. V., and Falzon, M. (2013) Parathyroid hormone-related protein regulates integrin α6 and β4 levels via transcriptional and post-translational pathways. *Exp. Cell Res.* **319,** 1419–1430
23. Danks, L., and Takayanagi, H. (2013) Immunology and bone. *J. Biochem.* **154,** 29–39
24. Sato, K., Suematsu, A., Nakashima, T., Takemoto-Kimura, S., Aoki, K., Morishita, Y., Asahara, H., Ohya, K., Yamaguchi, A., Takai, T., Kodama, T., Chatila, T. A., Bito, H., and Takayanagi, H. (2006) Regulation of osteoclast differentiation and function by the CaMK-CREB pathway. *Nat. Med.* **12,** 1410–1416
25. Negishi-Koga, T., and Takayanagi, H. (2009) Ca^{2+}-NFATc1 signaling is an essential axis of osteoclast differentiation. *Immunol. Rev.* **231,** 241–256
26. Suzu, S., Hiyoshi, M., Yoshidomi, Y., Harada, H., Takeya, M., Kimura, F., Motoyoshi, K., and Okada, S. (2007) M-CSF-mediated macrophage differentiation but not proliferation is correlated with increased and prolonged ERK activation. *J. Cell Physiol.* **212,** 519–525
27. Arai, A., Mizoguchi, T., Harada, S., Kobayashi, Y., Nakamichi, Y., Yasuda, H., Penninger, J. M., Yamada, K., Udagawa, N., and Takahashi, N. (2012) Fos plays an essential role in the upregulation of RANK expression in osteoclast precursors within the bone microenvironment. *J. Cell Sci.* **125,** 2910–2917
28. Sulpice, E., Ding, S., Muscatelli-Groux, B., Bergé, M., Han, Z. C., Plouet, J., Tobelem, G., and Merkulova-Rainon, T. (2009) Cross-talk between the VEGF-A and HGF signalling pathways in endothelial cells. *Biol. Cell* **101,** 525–539
29. Gherardi, E., Birchmeier, W., Birchmeier, C., and Vande Woude, G. (2012) Targeting MET in cancer: rationale and progress. *Nat. Rev. Cancer* **12,** 89–103
30. Inada, M., Matsumoto, C., Uematsu, S., Akira, S., and Miyaura, C. (2006) Membrane-bound prostaglandin E synthase-1-mediated prostaglandin E_2 production by osteoblast plays a critical role in lipopolysaccharide-induced bone loss associated with inflammation. *J. Immunol.* **177,** 1879–1885
31. Li, X., Udagawa, N., Takami, M., Sato, N., Kobayashi, Y., and Takahashi, N. (2003) p38 Mitogen-activated protein kinase is crucially involved in osteoclast differentiation but not in cytokine production, phagocytosis, or dendritic cell differentiation of bone marrow macrophages. *Endocrinology* **144,** 4999–5005
32. Miyaura, C., Inada, M., Matsumoto, C., Ohshiba, T., Uozumi, N., Shimizu, T., and Ito, A. (2003) An essential role of cytosolic phospholipase A2α in prostaglandin E2-mediated bone resorption associated with inflammation. *J. Exp. Med.* **197,** 1303–1310